by the methods of Winter et al.[13] and Gemmell et al.,[14] respectively. Male Wistar rats weighing about 150 g were used. Test compounds suspended in 5% arabic gum solution were administered orally 1 h before 1% λ-carrageenan (picnin A, Zushi Kagaku) and 1% zymosan (zymosan A, Sigma) in 0.1 mL of physiological saline (saline) were injected subplantarly into the hind paw. The paw volumes were measured by a plethsmograph immediately before the drugs were administered, and 3 and 4 h after carrageenan and zymosan were injected, respectively. The percentage of inhibition was calculated from the difference in mean swelling values between the test compounds treated animals and the control animals. This was then plotted versus the log of drug concentration and the value of ED_{40} or ED_{50} was estimated by linear-regression analysis.

Rabbit Anti-EA Antiserum. Rabbit anti-EA (egg albumin) antiserum was prepared according to the method of Koda et al.[15] Rabbits were immunized with an injection of a 1-mL suspension with an equal volume of saline containing EA (2 mg/mL) and FCA (Freund complete adjuvant), into each gluteus muscle at weekly intervals for 4 weeks. One week after the last immunization, the serum was obtained and pooled.

Reversed Passive Arthus Reaction-Induced Rat Paw Edema. This assay was conducted as described by Terasawa et al.[16] Male Wister rats weighing about 150 g were used. Test compounds suspended in 5% arabic gum solution were administered orally 1 h before EA injection. Thirty minutes after the administration of the compounds, 0.5 mL of rabbit anti-EA antiserum was injected into the tail vein. Thirty minutes later, 0.1 mL of saline containing 0.025 mg of EA was injected subplantarly into the hind paw. The paw volumes were measured by a plethsmograph immediately, before the drugs were administered and 2 h after EA injection. The percentage of inhibition was calculated from the difference in mean swelling values between the test compounds treated animals and the control group. This was then plotted versus the log of drug concentration, and the value of ED_{50} was estimated by linear-regression analysis.

Acute Toxicity. The compounds were orally administered to male dd mice weighing 20–25 g ($n = 3$). Minimum lethal doses (MLD) was determined by observing the mortality for 7 days after the administration.

Acknowledgment. We thank Dr. I. Miki and Dr. H. Nakajima for their assistance in the biochemical and pharmacological assays. We also thank K. Takada, Y. Watanabe, and A. Hata for their technical assistance and Dr. T. Hirata for encouragement and support.

Registry No. **9**, 139339-06-3; **10**, 139339-07-4; **11**, 139339-08-5; **12**, 139339-01-8; **13**, 139339-02-9; **14**, 139360-51-3; **15**, 139339-09-6; **16**, 139482-12-5; **17**, 139339-10-9; **18**, 141707-98-4; **19**, 139482-13-6; **20**, 139482-14-7; **21**, 139482-31-8; **22**, 139339-11-0; **23**, 139482-17-0; **24**, 139482-16-9; **25**, 141707-99-5; **26**, 139482-38-5; **27**, 139482-15-8; **28**, 139482-52-3; **29**, 139482-32-9; **30**, 139482-33-0; **31**, 139482-35-2; **32**, 139482-41-0; **33**, 139482-43-2; **34**, 139482-44-3; **35**, 139482-46-5; **36**, 139482-51-2; **37**, 139482-50-1; **38**, 139482-48-7; **39**, 139482-42-1; **40**, 139482-47-6; **41**, 139482-49-8; **42**, 139482-40-9; **43**, 139482-53-4; **44**, 139482-18-1; **45**, 139482-69-2; **46**, 141708-00-1; **46** free base, 139482-68-1; **47**, 141708-01-2; **47** free base, 139482-67-0; **48**, 139482-19-2; **49**, 139482-20-5; **50**, 139482-61-4; **51**, 139482-62-5; C_2H_5I, 75-03-6; *n*-C_3H_7I, 107-08-4; *i*-C_3H_7I, 75-30-9; $CH_2CHBrCH_2$, 4333-56-6; *n*-C_4H_9I, 542-69-8; *i*-C_4H_9I, 513-38-2; *n*-$C_6H_{13}I$, 638-45-9; $BrCH_2C_6H_5$, 100-39-0; $BrCH(CH_3)C_6H_5$, 585-71-7; $BrCH_2CH_2C_6H_5$, 103-63-9; $CH_2CHBrCHC_6H_5$, 36617-02-4; $BrCH_2$~cyclohexyl, 2550-36-9; $BrCH_2COCH_3$, 598-31-2; $BrCH_2CH_2CH_2OH$, 627-18-9; $BrCH_2CH_2OCH_2CH_3$, 592-55-2; $ClCH_2CO_2C_2H_5$, 105-39-5; $BrCH_2CH_2OCOCH_3$, 927-68-4; $BrCH_2$-4-ClC_6H_4, 622-95-7; $ClCH_2$-4-$NO_2C_6H_4$, 100-14-1; $BrCH_2$-4-$CH_3C_6H_4$, 104-81-4; $ClCH_2$-4-$CH_3OC_6H_4$, 824-94-2; $BrCH_2$-4-$CH_3O_2CC_6H_4$, 2417-72-3; $BrCH_2$-3-BrC_6H_4, 823-78-9; $BrCH_2$-3-$NO_2C_6H_4$, 3958-57-4; $BrCH_2$-3-$CH_3C_6H_4$, 620-13-3; $ClCH_2$-3-$CH_3OC_6H_4$, 824-98-6; $BrCH_2$-2-ClC_6H_4, 611-17-6; $ClCH_2$-2,5-$(CH_3)_2C_6H_3$, 824-45-3; $BrCH_2CO_2$*tert*-Bu, 5292-43-3; $BrCH_2CH_2CH_2Cl$, 109-70-6; propylene oxide, 75-56-9.

(13) Winter, C. A.; Risley, E. A.; Nuss, G. W. Carrageenin-Induced Edema in Hind Paw of the Rat as an Assay for Antiinflammatory Drugs. *Proc. Soc. Exp. Biol. Med.* **1962**, *111*, 544–547.
(14) Gemmell, D. K.; Cottney, J.; Lewis, A. J. Comparative Effects of Drugs on Four Paw Oedema Models in the Rat. *Agents Actions* **1979**, *9*, 107–116.
(15) Koda, A.; Nagai, H.; Wada, H. Pharmacological Actions of Baicalin and Baicalein. II. Active Anaphylaxis. *Folia Pharmacol. Jpn.* **1970**, *66*, 237–247.
(16) Terasawa, M.; Goto, K.; Maruyama, Y. Effect of Traxanox Sodium on Type I-IV Allergic Reactions. Studies on Anti-allergic Agent VII. *Folia Pharmacol. Jpn.* **1982**, *80*, 417–427.

Quenched Molecular Dynamics Simulations of Tuftsin and Proposed Cyclic Analogues

Stephen D. O'Connor, Paul E. Smith, Fahad Al-Obeidi, and B. Montgomery Pettitt*,†

Department of Chemistry, University of Houston, 4800 Calhoun Road, Houston, Texas 77204-5641.
Received September 3, 1991

We have used high-temperature quenched molecular dynamics calculations to investigate the conformational properties of tuftsin (Thr-Lys-Pro-Arg) in solution. Conformers obtained after quenching of the dynamical structures were sorted into families depending on their relative energies and backbone conformations. By examination of these families, several cyclic analogues of tuftsin were proposed and examined theoretically by further quenched dynamics simulations. Two of the four proposed analogues were found to adopt essentially identical conformations to that of linear tuftsin. It is suggested that these two derivatives (cyclo[Thr-Lys-Pro-Arg-Gly] and cyclo[Thr-Lys-Pro-Arg-Asp]) may be biologically active, and that the introduction of cyclic conformational constraints should help to reduce the entropic penalty to peptide binding.

Introduction

Tuftsin is a linear tetrapeptide (Thr-Lys-Pro-Arg) which is involved in the stimulation of the phagocytosis of polymorphogranulocytes and phagocytes.[1] Tuftsin is located between residues 289 and 292 of the heavy chain of leukokinin (a cytophilic γ-globulin),[2] in the sequence -Val-His-Asn-Ala-Lys-*Thr-Lys-Pro-Arg*-Glu-Gln-Gln-Tyr-Asx-, and in close proximity to the carbohydrate binding region.[3]

† Alfred P. Sloan Fellow 1989–91.

(1) Fridkin, M.; Gottlieb, P.; Tuftsin, Thr-Lys-Pro-Arg. *Mol. Cell. Biochem.* **1981**, *41*, 73–97.
(2) Najjar, V. A.; Nishioka, K. Tuftsin: A natural phagocytosis stimulating peptide. *Nature* **1970**, *228*, 672–673.

0022-2623/92/1835-2870$03.00/0

Complete release of this tetrapeptide from the carrier molecule occurs in two stages. Firstly, cleavage of the Arg-Glu peptide bond by a splenic enzyme, *tuftsin endocarboxy peptidase*, produces leukokinin-S containing the free carboxyl terminus of tuftsin. Secondly, after leukokinin-S is bound to the blood and tissue granulocyte by the membrane enzyme *leukokininase*, the Lys-Thr peptide bond is cleaved. Therefore, after a splenectomy, no release of tuftsin can occur and phagocytosis is impaired.[4]

Since its discovery,[2] tuftsin has been the subject of several theoretical and experimental studies aimed at determining the important biologically active conformation(s), and explaining the observed structure–activity relationships.[5] The tuftsin fragment has been shown to be responsible for the full observed activity and any modification in the sequence, by either deletion or addition, results in either loss of activity or inhibitory activity in the stimulation of phagocytosis.[6]

It is well appreciated that flexible biological molecules (such as linear peptides) probably exist in numerous low-energy states in solution,[7,8] and a particular (active) conformation may only be obtained upon interaction with a specific receptor.[9] It is also common practice to use synthetic conformational constraints to investigate the details of the active conformation of flexible peptides.[10,11] These constraints help to limit the large number of conformations available to linear peptides in solution, therefore reducing the entropic penalty to the binding free energy. It should be feasible to adopt this type of approach in developing more potent analogues of tuftsin.

The strategy employed here was to use high-temperature quenched molecular dynamics (QMD) to search the conformational space available to tuftsin in solution. The structures generated by the high-temperature dynamics were minimized and subsequently divided into families according to their relative energies and conformational properties. The families obtained for linear tuftsin were then used as the basis for several proposed cyclic analogues of tuftsin. Each of the analogues was subjected to a separate quenched dynamics run to search the local conformational space of the new cyclic peptides. If the cyclic analogues displayed similar conformational properties to the parent compound, it is suggested that the analogue will have similar, or hopefully improved, activity due to the reduced entropic contribution to binding as facilitated by ring closure.

At this point, it is worth mentioning a closely related procedure known as simulated annealing (SA),[12] which has also been used to search the conformational space of small peptides.[13-15] Most applications of SA involve a Monte Carlo search of conformational space using an acceptance criterion corresponding to a high temperature (~1000 K). In this way, SA and QMD are similar. However, whereas in QMD the individual structures from the trajectory would be minimized to produce an ensemble of structures, in SA the temperature is gradually decreased until the system "freezes" to a single structure. If an infinitely slow cooling rate is used, the procedure should converge to the global minimum-energy structure.[12] Unfortunately, such a cooling rate is impractical, and a satisfactory cooling procedure is often a matter of trial and error.[14] More importantly, we were interested in the distribution of low-energy (thermally accessible) conformers rather than a single minimum-energy structure.

As only a few implementations of QMD exist, we have also performed two preliminary control studies. The first control concentrates on the problem of conformational sampling and the use of an energy cutoff to obtain the most probable conformations. For this control we used 2-bromobutane which has only one interesting degree of freedom, and can therefore be studied analytically as well as by simulation. The second control involved QMD of the Met-enkephalin pentapeptide, and subsequent comparison of the resultant structures with the closely related cyclic analogue, DPDPE. Previous studies have shown the enkephalin derivative DPDPE, Tyr-cyclo[(D)Pen-Gly-Phe-(D)Pen], to be a very potent and selective inhibitor of the δ-opioid receptor.[16] It has been extensively studied, both experimentally[17,18] and theoretically,[17,19-21] and a

(3) Edelman, G. M.; Cunningham, B. A.; Gall, W. E.; Gottlieb, P. D.; Rutishauser, U.; Waxdal, M. J. The covalent structure of an entire γ-G immunoglobulin molecule. *Proc. Natl. Acad. Sci. U.S.A.* **1969**, *63*, 78–85.

(4) Najjar, V. A. In *The Reticuloendothelial System: A Comprehensive Treatise*, Sbarra, A. J., Strauss, R. R.; Eds.; Plenum Press: New York, 1980; Vol. 2, pp 45–71.

(5) Siemion, I. Z.; Konopinska, D. Tuftsin analogs and their biological activity. *Mol. Cell. Biochem.* **1981**, *41*, 99–112.

(6) Fridkin, M.; Stabinsky, Y.; Zakuth, V.; Spirer, Z. Tuftsin and some analogs. Synthesis and interaction with human polymorphonuclear Leukocytes. *Biochim. Biophys. Acta* **1977**, *496*, 203–211.

(7) Pettitt, B. M.; Karplus, M. Interaction Energies. In *Molecular Graphics and Drug Design*; Burgen, A. S. V., Roberts, G. C. K., Tute, M. S.; Eds.; Elsevier Science, B. V.: New York, 1986; pp 75–113.

(8) van Gunsteren, W. F.; Berendsen, H. J. C. Computer simulation of molecular dynamics: Methodology, applications and perspectives in chemistry. *Angew. Chem., Int. Ed. Engl.* **1990**, *29*, 992–1023.

(9) Pettitt, B. M.; Matsunaga, T.; Al-Obeidi, F.; Gehrig, C.; Hruby, V. J.; Karplus, M. Dynamical Search for Bis-Penicillamine Enkephalin Conformations: Quenched Molecular Dynamics. *Biophys. J.*, in press.

(10) Hruby, V. J.; Al-Obeidi, F.; Kazmierski, W. *Biochem. J.* **1990**, *268*, 249–262.

(11) Degrado, W. F. Design of peptides and proteins. *Adv. Protein Chem.* **1988**, *39*, 51–124.

(12) Kirkpatrick, S.; Gelatt, C. D.; Vecchi, M. P. Optimization by simulated annealing. *Science* **1983**, *220*, 671–680.

(13) Wilson, S. R.; Cui, W. Application of simulated annealing to peptides. *Biopolymers* **1990**, *29*, 225–235.

(14) Nayeem, A.; Vila, J.; Scheraga, H. A. A comparative study of the simulated annealing and Monte Carlo-with-minimization approaches to the minimum-energy structures of polypeptides: [Met]-enkephalin. *J. Comput. Chem.* **1991**, *12*, 594–605.

(15) Morales, L. B.; Garduno-Juarez, R.; Romero, D. *J. Biomol. Struct. Dyn.* **1991**, *8*, 721–735.

(16) Mosberg, H. I.; Hurst, R.; Hruby, V. J.; Yamamura, K. G. H. I.; Galligan, J. J.; Burks, T. F. Bis-Penicillamine enkephalins possess highly improved specificity toward δ-opioid receptors. *Proc. Natl. Acad. Sci. U.S.A.* **1983**, *80*, 5871–5874.

(17) Hruby, V. J.; Kao, L.; Pettitt, B. M.; Karplus, M. The conformational properties of the delta opioid peptide bis-d-penicillamine enkephalin in aqueous solutions determined by NMR and energy minimization calculations. *J. Am. Chem. Soc.* **1988**, *110*, 3351–3359.

(18) Mosberg, H. I.; Sobczyk-Kojiro, K.; Subramanian, P.; Crippen, G. M.; Ramalingam, K.; Woodward, R. W. Combined use of stereospecific deuteration, NMR, distance geometry and energy minimization for the conformational analysis of the highly δ opioid receptor selective peptide [D-pen^2,D-pen^5]enkephalin. *J. Am. Chem. Soc.* **1990**, *112*, 822–829.

(19) Nikiforovich, G. V.; Balodis, J.; Shenderovich, M. D.; Golbraikh, A. A. Conformational features responsible for binding of cyclic analogs of enkephalin to opioid receptors. *Int. J. Pept. Protein Res.* **1990**, *36*, 67–78.

(20) Smith, P. E.; Dang, L. X.; Pettitt, B. M. Simulated Structure and Dynamics of the Bis-Penicillamine Zwitterion. *J. Am. Chem. Soc.* **1991**, *113*, 67–73.

(21) Smith, P. E.; Pettitt, B. M. Effects of Salt on the Structure and dynamics of the Bis(penicillamine) Enkephalin Zwitterion: A Simulation Study. *J. Am. Chem. Soc.* **1991**, *113*, 6029–6037.

structure consistent with the available NMR data has been proposed.[17] The families of Met-enkephalin obtained from QMD were compared with the known structure of DPDPE to establish the validity of the approach. Therefore, if a successful comparison can be made between the QMD structures of Met-enkephalin and DPDPE, then this technique may be useful in the design of superpotent analogues for other naturally occurring peptides.

Method

All calculations were performed with the CHARMM program using the parameter set employing an extended atom representation for nonpolar hydrogens.[22] The equations of motion were integrated using the Verlet algorithm[23] with a time step if 1 fs and SHAKE[24] to constrain all bond lengths. The influence of the solvent environment was modeled by a dielectric continuum employing a dielectric constant of either 45, representative of dimethyl sulfoxide (DMSO), or 80, to represent aqueous media. While packing effects can be significant, the dominant effect on the energy surface has been shown to be due to dielectric screening in polar solvents.[7,25] The advantages and shortcomings of continuum models have been well-studied,[25] and such a model should suffice for the purpose of this study.

The same approach was adopted for all of the peptides studied. Initially, the fully extended zwitterionic structure of Met-enkephalin or tuftsin was minimized. The peptide was then heated to 1000 K over 10 ps of dynamics by incrementing the temperature 10 K every 100 time steps (0.1 ps). After heating, the peptide was equilibrated for an additional 10 ps at 1000 K, during which a ±13 K constraint in temperature was applied to the system. The molecular dynamics production runs were then performed in the microcanonical (NVE) ensemble for a total time of 2 ns (Met-enkephalin control), 600 ps (linear tuftsin), and 150 ps (cyclic tuftsin analogues). The trajectories were saved every 1 ps.

Each of the saved structures were thoroughly energy minimized using 1000 steps of steepest decent followed by 1000 steps of adopted basis Newton–Raphson, giving a rms energy derivative of ≤0.001 kcal mol per Å. For the extended run of Met-enkephalin, several cis peptide bonds were observed. These peptide bond flips were a direct consequence of the force field and high temperature used and did not suggest any physical peptide bond isomerization. Hence, during the minimization procedure a harmonic potential (force constant of 50 kcal/mol per rad^2) was applied to each of the ω dihedrals of Met-enkephalin, ensuring all the peptide bonds adopted the normal trans conformation.

In general, the structures obtained for each peptide displayed a Gaussian-like (bell-shaped) distribution of energies, the low-energy tail of the distribution being representative of those conformers which would be more probable in solution. Therefore, only those structures within ~3–5 kcal/mol of the minimum energy were considered for further analysis. Each of these selected structures were then analyzed according to their backbone (ϕ,ψ) conformational distributions and sorted into families by computing the rms difference between the C$^\alpha$–C backbone fragments of each residue over all the structures. Structures with an rms deviation of ≤0.6 Å were considered to be members of the same family. It should be noted that including more backbone atoms in the fitting procedure did not significantly alter the results.

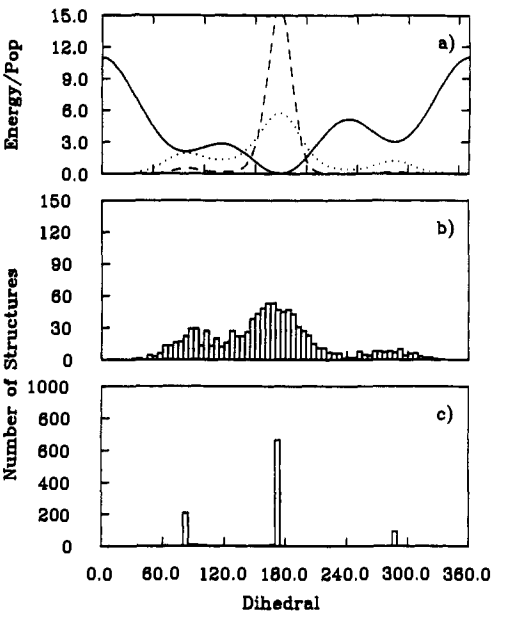

Figure 1. (a) Adiabatic map of the 2-bromobutane dihedral (solid line). Energy in kilocalories/mole. Calculated Boltzmann-weighted percentage population at 300 K (dashed line) and 982 K (dotted line). (b) Histogram of the observed dihedral angles before minimization. (c) Histogram of the dihedral angles after minimization.

Results and Discussion

In this section we present the results of our conformational searches. The results for 2-bromobutane are presented as a test of the ability of QMD to correctly reproduce a known conformational population distribution. As a further test we have applied the technique to Met-enkephalin, which is known to have several highly potent synthetic analogues including the bis-penicillamine analogue (DPDPE).

(a) (*S*)-2-Bromobutane. 2-Bromobutane was chosen because the torsional potential energy surface possesses three unequal minima and the torsional population distribution is easily calculated at any temperature, both analytically and numerically via simulation. The system was simulated for a total of 1 ns after an initial velocity assignment and 10 ps of equilibration at 1000 K. The average temperature during the 1 ns of production was 956 ± 302 K. The structures obtained every picosecond were saved for further analysis. Figure 1a shows the underlying potential energy surface for rotation around the dihedral angle of 2-bromobutane. Also shown in Figure 1a are the Boltzmann-weighted population distributions calculated at both 300 and 956 K from the potential surface. Using the C–C–C–Br dihedral potential (and assuming the usual definitions of g^-, g^+, and t) the population of each of the conformers was calculated to be g^- (12%), g^+ (23%), t (65%) at 982 K and g^- (1%), g^+ (4%), t (95%) at 300 K.

A histogram of the dihedral angles of the 1000 unminimized structures is displayed in Figure 1b. As expected, this distribution closely resembled the calculated popu-

(22) Brooks, B. R.; Bruccoleri, R. E.; Olafson, B. D.; States, D. J.; Swaminathan, S.; Karplus, M. CHARMM: A program for macromolecular energy, minimization, and dynamics calculations. *J. Comput. Chem.* **1983**, *4*, 187–217.
(23) Verlet, L. Computer "experiments" on classical fluids. 1. Thermodynamical properties of Lennard-Jones molecules. *Phys. Rev.* **1967**, *159*, 98–103.
(24) Ryckaert, J. P.; Ciccotti, G.; Berendsen, H. J. C. Numerical integration of the Cartesian equations of motion of a system with constraints: Molecular dynamics of n-alkanes. *J. Comput. Phys.* **1977**, *23*, 327–41.
(25) Pettitt, B. M.; Rossky, P. J. Modeling of Solvation Effects in Biopolymer Solutions. *Theor. Biochem. Mol. Biophys.*; Beveridge, D. L.; Lavery, R.; Eds.; Academic Press: New York, 1990; pp 1–7.

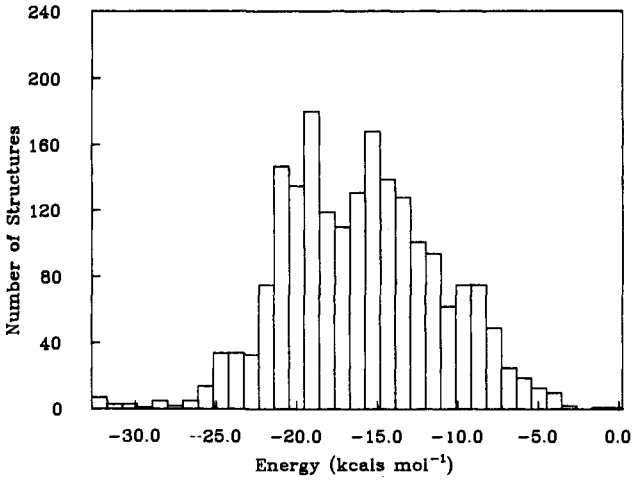

Figure 2. An energy histogram of the 2000 structures of Met-enkephalin generated from a 2-ns dynamics simulation after energy minimization.

lation distribution at 956 K. After minimization of all the structures, one obtains the distribution shown in Figure 1c. This corresponded to conformational populations of g^- (10%), g^+ (22%), and t (68%), which are essentially those predicted for 956 K. By using an energetic sieve one can discard the conformers which have small populations at 300 K, thereby recovering a distribution which more closely resembles such a temperature. Using a cutoff energy of ~3 kcal/mol would select all the conformations in the g^+ and t wells. Using a cutoff of 2 kcal/mol would yield only the trans conformers. Hence, high-temperature QMD with an appropriate sieve may be used to adequately sample the width of the population distribution available to 2-bromobutane at normal temperatures. While the populations of the less probable conformers are somewhat exaggerated with this sieved-QMD technique, the width of the overall distribution (i.e. number of conformers available) is more representative of the lower-temperature system thatn the high-temperature one. Thus, the technique effectively explores the available conformational space and, by using an energetic criterion, can select the relevant conformers representative of a lower temperature.

(b) Met-enkephalin (Tyr-Gly-Gly-Phe-Met). An important requirement for any conformational search procedure is that it ensures good sampling of conformational space. A 2-ns QMD simulation was performed for Met-enkephalin in a continuum dielectric representation of water, producing 2000 structures for analysis. After minimization the 2000 structures ranged in energy between −32.7 and 0.2 kcal/mol with a mean of −16.0 kcal/mol (see Figure 2). Figure 3 displays the ϕ,ψ and χ^1,χ^2 dihedral maps obtained from structures generated at 10-ps intervals during the run. It should be noted that this represented only 10% of the total number of structures analyzed, and 0.01% of the total number of structures generated, and that very high energy conformations were removed by the minimization procedure. From the spread in the figures, it is clear that the peptide explored a great proportion of the conformational space available to it.

Selecting structures with an energy lower than −26.0 kcal/mol, and then grouping them into families based on

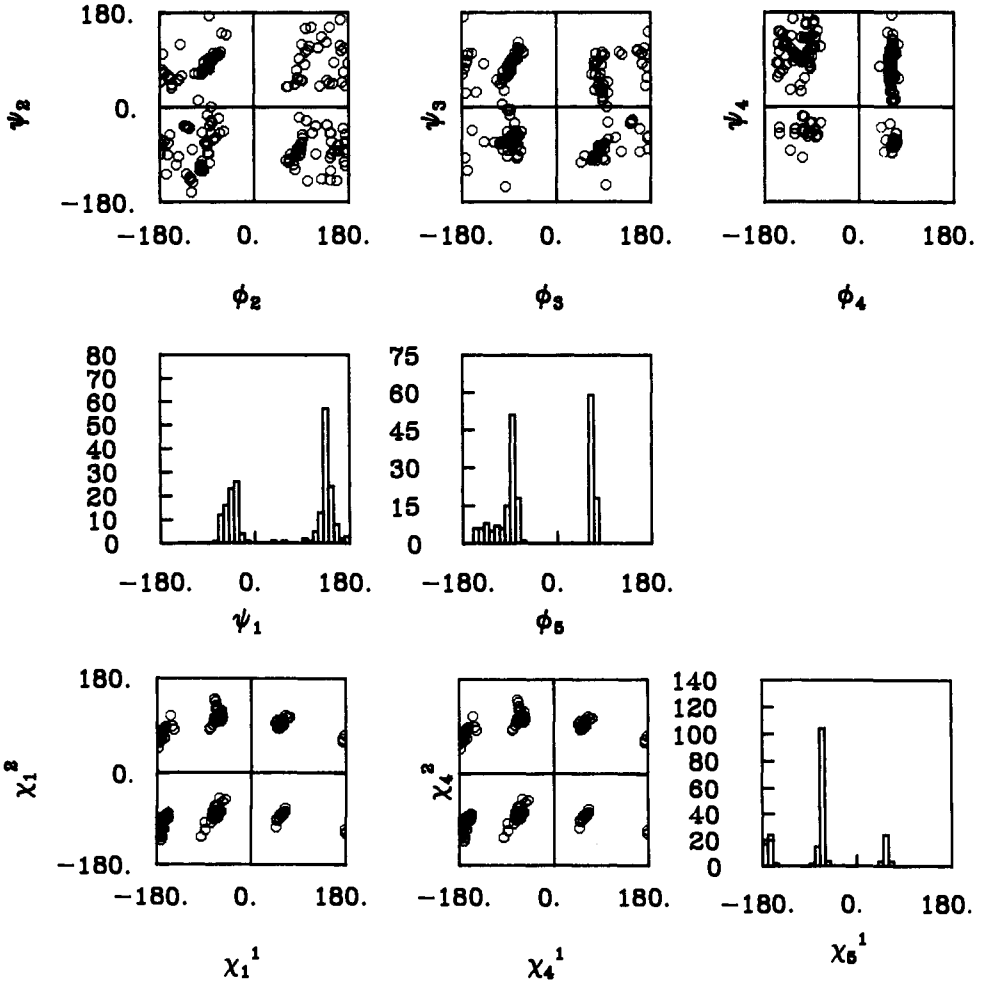

Figure 3. ϕ,ψ and χ^1,χ^2 maps and histograms for 200 structures of Met-enkephalin. The structures were generated at 10-ps intervals during a 2-ns quenched molecular dynamics simulation in water.

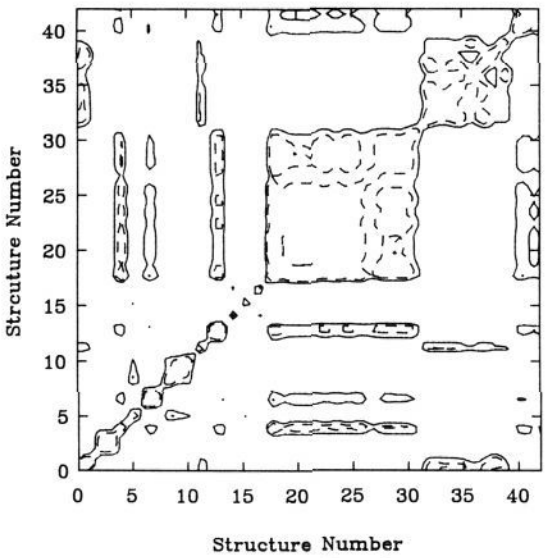

Figure 4. The rms deviation between the 42 low-energy structures of Met-enkephalin. The structure number is representative of the time development of the low-energy structures. Structure 0 is the initial conformation and structure 42 is the last low-energy structure generated, as determined by the energy cutoff criterion. The solid contour corresponds to an rms deviation of 0.6 Å and the broken line to 0.3 Å.

the rms deviation between each of the structures, yielded 42 selected structures in five different families. The cross correlation of the rms deviation between the selected structures is displayed as a contour plot in Figure 4, the off diagonal intensity indicating structures which were closely related. Table I lists the ϕ,ψ and χ dihedral angles which were representative of each of the three main families, together with a previously proposed conformation of DPDPE which is consistent with much of the available NMR data.[17]

Selected low-energy conformers from each of the three main families were studied graphically, with particular emphasis given to the representatives from families 1 and 2 since they were the most highly populated and had relative energies much lower than the other families. Only one structure that was analyzed adopted a linear conformation with a large separation between the N and C termini. All the other structures adopted pseudomacrocyclic conformations with hydrogen bonds involving the two terminal groups. In all three families there was a tendency for the amide dipoles to align rather than oppose each other.[20] Neglecting ψ_1 and ϕ_5 (which are not part of the macrocycle of DPDPE and are therefore expected to have free rotation), the agreement between the major structural elements of family 1 and DPDPE was excellent.

The first family was characterized by three hydrogen bonds from each of the NH's of Tyr-1, Gly-2, and Gly-3 to the carboxylate terminus. All side chains were located on the same side of the pseudomacrocycle. In the second family, there were hydrogen bonds between the NH of Tyr-1 and the CO of Phe-4, and also between the NH of Gly-2 and the CO of Phe-4. The aromatic rings of Tyr and Phe were also positioned on the same side of the pseudomacrocycle. The third family possessed hydrogen bonds between the N and C termini, the NH of Gly-2 and the C terminus, as well as between the NH of Met-5 and the CO of Gly-2. Again, the aromatic rings were positioned on the same side of the pseudomacrocycle, although they were further apart than in the first two families.

Table I. Representative Dihedral Angles of Met-enkephalin and DPDPE from Quenched Molecular Dynamics in Water

residue	dihedral	F1	F2	F3	DPDPE
Tyr-1	ψ	−36	−36	−35	164
	χ^1	56	51	52	−163
	χ^2	−85	85	−93	51
Gly-2 or (D)Pen-2	ϕ	128	−164	−134	111
	ψ	41	−90	69	14
	χ^1				−180
	χ^2				143
	χ^3				−110
Gly-3	ϕ	−145	−75	68	−98
	ψ	−96	−55	−97	−18
Phe-4	ϕ	−89	−100	−81	−72
	ψ	−46	157	−34	−46
	χ^1	−62	−178	−175	179
	χ^2	104	−121	69	68
Met-5 or (D)Pen-5	ϕ	−103	−91	−78	83
	χ^1	−63	−68	−69	−70
	χ^2	180	−63	62	119
	χ^3	90	110	87	
no. in family		22	11	5	
energy (kcal/mol)		−32.7	−28.5	−27.0	

The minimum-energy structures from the two main families were compared to an average NMR structure of DPDPE by performing an rms fit of all the main-chain atoms between the C^α of residue 1 and the C^α of residue 5. Once superimposed, families 1 and 2 displayed a remarkable conformational similarity to the model-built NMR structure.[17] The total rms difference between the main-chain of family 1 and that of the DPDPE model was 1.54 Å, while family 2 gave a 1.33-Å difference. These differences were small, especially when one considers that DPDPE contains two residues possessing D chirality, rather than all L as in Met-enkephalin, and is also constrained by a disulfide bond. A graphical comparison of the model-built DPDPE and the minimum-energy structure from family 2 (see Figure 5) shows that not only did the main chains match quite well but the Tyr and Phe rings were also in identical positions. Rotation around χ^2 of Phe, which is very facile in solution, would increase the agreement between the structures even more. As the relative positions of the tyrosine ring and the pseudomacrocycle are thought to be essential to binding,[26] these observations

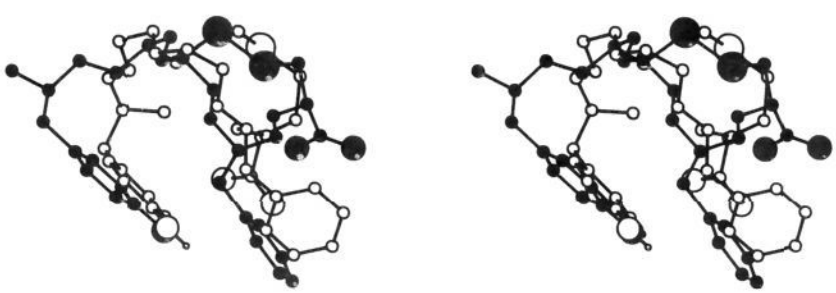

Figure 5. A stereo plot comparing the lowest energy structure from family 2 of Met-enkephalin (open spheres) with a proposed solution conformation of DPDPE (shaded spheres). Only the backbone (N, C^α, and C) and some side-chain atoms are shown for clarity.

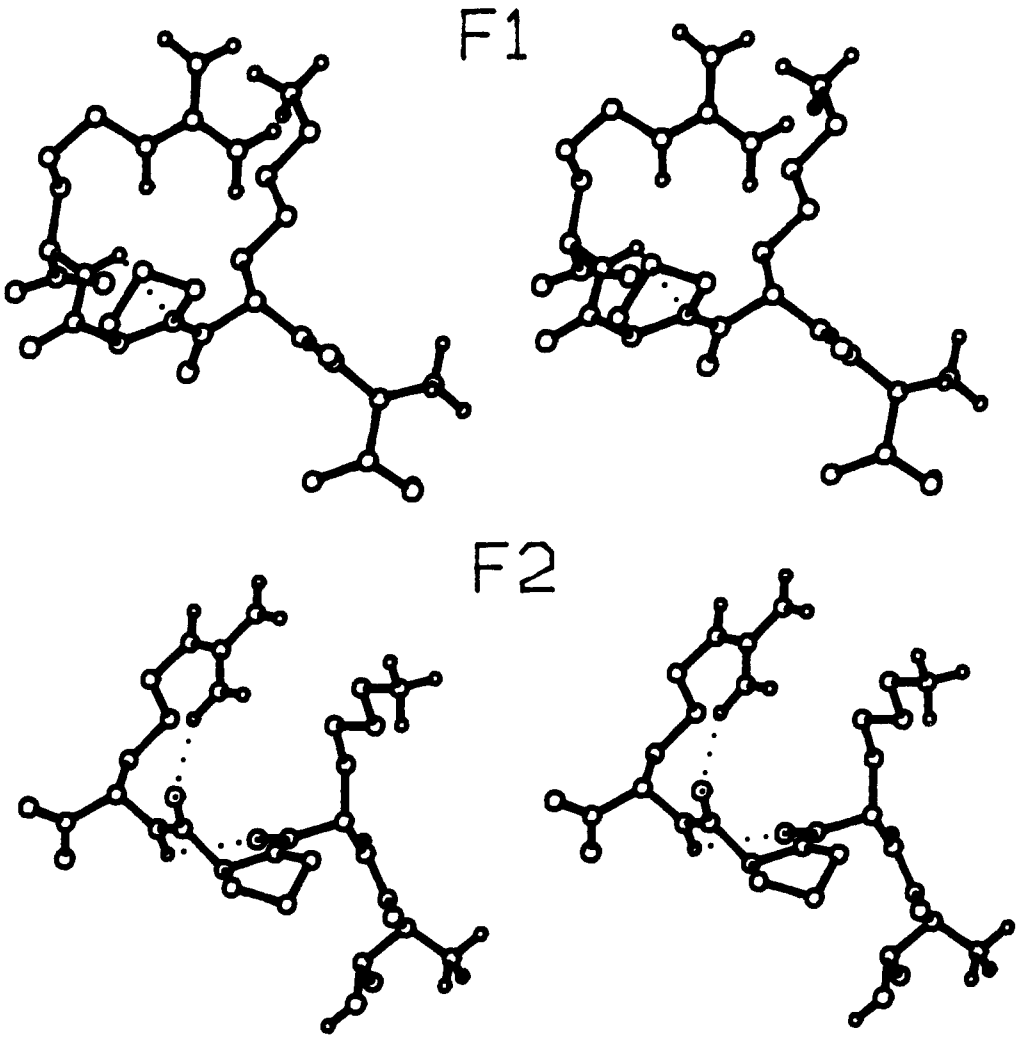

Figure 6. Stereo plots of representative structures from families 1 and 2 of tuftsin in DMSO generated by quenched molecular dynamics.

were very encouraging. We feel that the folded structures obtained here, generated from a fully extended initial conformation of Met-enkephalin, provide reasonable justification that this type of approach can yield useful results in the search for possible active conformations of tuftsin in solution.

Simulated annealing, its variants, and other methods have been used to locate the minimum-energy structure for a different protonation state of Met-enkephalin.[14,15] While the observed structures from those studies display important differences compared with the lowest energy structure from our QMD simulations, the former studies used a different force field (ECEPP/2) and, more importantly, treated the peptide termini as neutral groups rather than the charged (zwitterionic) groups used here. As a test we used a previously observed global energy minimum for a different potential,[14] and then minimized using the zwitterionic form of the peptide and the same dielectric conditions as used in the present QMD runs. The resulting structure was ~3 kcal/mol higher in energy than our minimum.

(c) Linear Tuftsin (Thr-Lys-Pro-Arg). Using the same technique, we now turn our attention to tuftsin, the object of this study. The QMD simulation of tuftsin in a dielectric continuum representation of DMSO, and subsequent minimization, generated an ensemble of 42 structures with energies within 3 kcal/mol of the energy minimum. Regrouping these 42 conformers, according to the rms deviations between their C^{α}–C fragments, produced four families of structures which are shown in Table II. Among the four families there was one major family (F1) and three additional minor families. Family 1 possessed a type IV β-turn[27] backbone conformation with one

Table II. Representative Dihedral Angles of Tuftsin from Quenched Molecular Dynamics in DMSO

residue	dihedral	F1	F2	F3	F4
Thr-1	ψ	129	146	-43	-56
	χ^1	-58	55	55	-58
	χ^2	-62	179	179	-62
Lys-2	ϕ	-83	-85	-89	-81
	ψ	134	124	127	134
	χ^1	-66	-169	-173	42
	χ^2	-177	66	-179	69
Pro-3	ϕ	-68	-65	-77	-70
	ψ	-22	94	-164	123
	χ^1	28	-28	35	-29
Arg-4	ϕ	-82	-118	-71	-78
	χ^1	-61	-71	-66	-69
	χ^2	135	-66	-67	74
no. in family		38	1	2	1
energy (kcal/mol)		-8.36	-6.75	-8.66	-7.89

(26) Hruby, V. J.; Pettitt, B. M. Conformational-Biological Activity Relationships for Receptor Selective, Conformationally Constrained Opioid Peptides. In *Computer-aided Drug Design: Methods and Applications*; Perun, T. J., Propst, C. L.; Eds.; Marcel Dekker: New York, 1989; pp 405–460.

(27) Lewis, P. N.; Momany, F. A.; Scheraga, H. A. Chain reversals in proteins. *Biochim. Biophys. Acta* **1973**, *303*, 211–229.

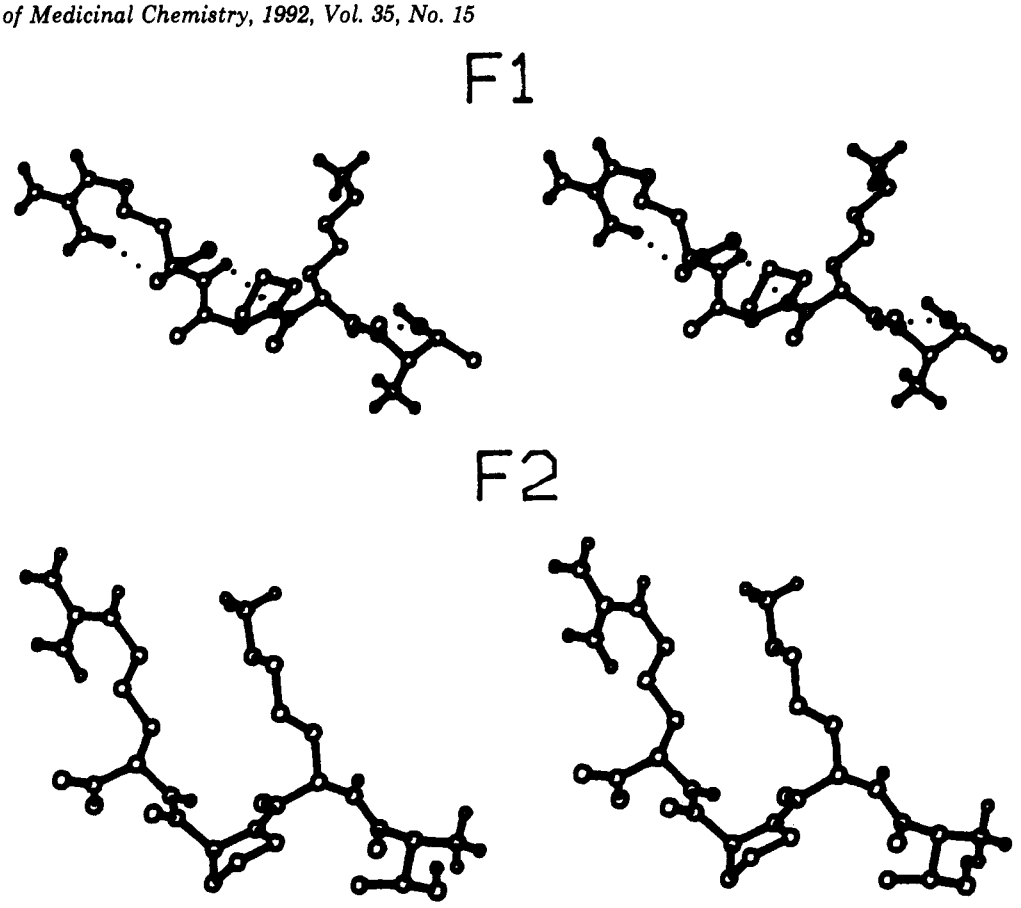

Figure 7. Stereo plots of representative structures from families 1 and 2 of tuftsin in water generated by quenched molecular dynamics.

hydrogen bond between the Pro-3 N and Arg-4 NH (F1 in Figure 6). All the side-chain conformations adopted the preferred g^- and t orientations. Within the main family the structures maintained a constant backbone conformation but displayed some side-chain differences which may explain the range of their total energies.

The χ^1 dihedral angle of Thr-1 adopted a g^+ conformation in two of the families (F2, F3). Although g^+ is a less favorable conformation, a hydrogen bond between Thr-1 OH and Lys-2 NH provided extra stabilization for this conformation. The χ^1 dihedral of Pro-3 was also observed in a g^+ conformation which is typical of a twisted pyrrolidine ring conformation. Both the Lys-2 and Arg-4 side chains usually occupied the more favorable g^- and t conformations and were located on the same face of the molecule. This distribution of polar groups may be related to the biological activity of tuftsin. It has been reported that replacement of Lys or Arg, by either L amino acid isosteres or D isomers, leads to complete loss of tuftsin's enhancement of the phagocytosis of macrophages.[28,29] This loss in biological activity could be related to changes in the conformation of the polar side chains of Lys and/or Arg, or due to the change of net charge on the peptide.

Examination of the conformational families generated in a continuum aqueous solvent revealed one major family and two additional minor ones (Table III). Family 1 displayed a total of three short-range hydrogen bonds, i.e. hydrogen bonds between two neighboring residues or within the same residue (see F1 in Figure 7). The general backbone conformation of family 1 was a type IV β-turn. This family of structures conflicts with previously reported theoretical results.[30,31] The side-chain segregation displayed an amphiphilic type of structure,[32] with the Thr-1, Lys-2, and Arg-4 side chains situated on one side of the molecule away from the proline ring. The puckering observed for the pyrrolidine ring was of C_2 symmetry (half-chair or twist) with respect to the backbone conformation. As the range of observed ϕ values for Pro in protein crystal structures is $-65 \pm 15°$,[33] this conformation

Table III. Representative Dihedral Angles of Tuftsin from Quenched Molecular Dynamics in Water

residue	dihedral	F1	F2	F3
Thr-1	ψ	-48	129	147
	χ^1	55	-58	54
	χ^2	64	-62	64
Lys-2	ϕ	-88	-91	-110
	ψ	126	122	113
	χ^1	-64	-174	-177
	χ^2	179	-176	80
Pro-3	ϕ	-69	-75	-74
	ψ	-31	79	164
	χ^1	30	33	31
Arg-4	ϕ	-105	-87	-86
	χ^1	-166	33	-59
	χ^2	-91	-169	-70
no. in family		40	4	1
energy (kcal/mol)		-9.99	-8.92	-8.41

(28) Nawrocka, E.; Siemion, I. Z.; Slopek, S.; Szymaniec, S. Tuftsin analogs with D-amino acid residues. *Int. J. Pept. Protein Res.* **1980**, *16*, 200–207.
(29) Sucharda-Sobczyk, A.; Siemion, I. Z.; Nawrocka, E. The influence of configuration changes in tuftsin peptide chain on its folding properties. *Acta Biochim. Pol.* **1980**, *27*, 353–363.
(30) Fitzwater, S.; Hudes, Z. I.; Scheraga, H. A. Conformational energy study of tuftsin. *Macromolecules* **1978**, *11*, 805–811.
(31) Nikiforovich, G. V. *Bioorg. Khim.* **1978**, *4*, 1427–1431.
(32) Kaiser, E. T.; Kezdy, F. J. Amphiphilic secondary structure: Design of peptide hormones. *Science* **1984**, *223*, 249.
(33) Symersky, J.; Blaha, K.; Jecny, J. Structure of *cyclo* Tri-D-azetidine-2-carboxylic acid. *Acta Crystallogr.* **1988**, *C44*, 148–150.

F1

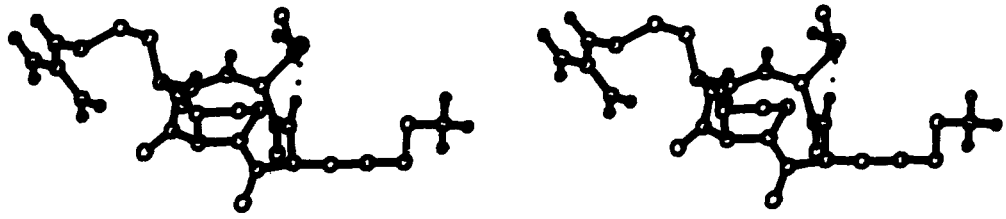

Figure 8. Stereo plot of a representative structure for $ctuf_1$ in DMSO generated by quenched molecular dynamics.

was within the allowed region of conformational space available to the proline backbone in position 3 of a β-turn.[34] The proline ψ dihedral in family 3 was consistent with a collagen (polyproline) conformation of 155 ± 10°.

There were some slight differences between the structures obtained from the DMSO and aqueous continuum solvent studies. Some of the higher energy members of both major families displayed similar backbone conformations but differed in their side-chain arrangement and the absence of any short-range hydrogen bonds (Table II and Figure 6 vs Table III and Figure 7). In general, the predicted backbone conformations of tuftsin in DMSO were similar to those from the aqueous study, except for the absence of a few hydrogen bonds found in the latter. Thus, the change in solvent dielectric appeared to have only minor effects on the backbone conformation of tuftsin. NMR studies of tuftsin support a more ordered β-turn structure for tuftsin in DMSO (vs a random structure in aqueous media) as determined by the low sensitivity of the change in chemical shift with respect to temperature ($\Delta\delta/\Delta T$) for the Arg-4 NH proton.[35] During our simulations, the Arg-4 NH proton maintained a high degree of solvent accessibility in both solvents.

Earlier studies suggest that one probable conformation of tuftsin involves a β-turn with a hydrogen bond located between Thr and Arg.[36] However, this is not corroborated by NMR studies in solution.[35] Using theoretical calculations, other workers have concluded that, in the bioactive conformation(s) of tuftsin, the Lys-2 NH_3 group is in close proximity to the carboxylate terminus (quasi-cyclic model).[31] On the basis of this finding, a cyclic analogue was synthesized which, unfortunately, possessed reduced potency relative to native tuftsin.[37] In contrast, we found that the Lys-2 NH_3 to carboxylate terminus distance distribution was very similar to the Thr-1 NH to carboxylate terminus distribution. Other theoretical studies by Fitzwater et al.[30] suggested that tuftsin adopts a C_7^{eq} conformation with a possible cis Lys-Pro peptide bond. In our study, the Lys side chain was always oriented away from the carboxylate terminus and no cis proline peptide bond was observed in any of the selected conformers (nb. no constraints were applied during the minimization procedure). The absence of a cis Lys-Pro peptide bond is supported by NMR studies of tuftsin in both water and DMSO.[35] A few of the conformers did adopt a C_7^{eq} conformation although this was a minor conformation in the selected structures studied here. The depopulation of the C_7 conformation in water is consistent with more robust computer simulations of peptides using an explicit molecular representation of the aqueous environment and with many-body theories.[38,39]

(d) Cyclic Tuftsin Analogues. Our work suggests that one of the major conformational families of tuftsin involves a type IV β-turn with the Lys and Arg side chains positioned on the same face of the molecule. Previous experimental work reported that slight changes in the tetrapeptide primary sequence can result in a reduction or total loss of biological activity.[1,5] It has also been reported that tuftsin loses little potency when a Gly is concatenated to the end of the sequence.[40] On the basis of these findings the following four cyclic peptides were designed and subjected to further theoretical analysis. The analogues were designed in order to test some of the possible ring sizes and peptide sequences which will adopt the same type IV β-turn and side-chain orientations as linear tuftsin. The analogues are $ctuf_1$ = cyclo[Thr-Lys-Pro-Arg], $ctuf_2$ = cyclo[Thr-Lys-Pro-Arg-Gly], $ctuf_3$ = cyclo[Thr-Lys-Pro-Arg-Lys], and $ctuf_4$ = cyclo[Thr-Lys-Pro-Arg-Asp].

First, simple cyclization of the peptide between the N and C terminal groups (via a lactam ring) was considered ($ctuf_1$). This seemed to be an appropriate starting point for our theoretical studies. Second, since most of the selected conformers of tuftsin exhibited distances between the N and C termini of ≥6 Å, it seemed reasonable that a lactam cyclization of Thr-Lys-Pro-Arg-Gly, which has an extra glycine and could decrease this distance to ~2 Å, would lower the strain induced in the system upon cyclization and may therefore possess similar conformational characteristics to linear tuftsin ($ctuf_2$). Finally, we investigated the effect of varying the total charge on the peptide by addition of charged residues to the end of the sequence. Both the Lys and Arg residues of tuftsin contribute a +1 charge to the total charge on the peptide, resulting in a net charge of +2 at physiological pH. The final two peptides were proposed in order to expore modifications of this total charge. The addition of a Lys

(34) Chandrasekaran, R.; Lakshminarayan, A. V.; Pandya, U. V.; Ramachandran, G. N. Conformation of the LL and LD hairpin bends with internal hydrogen bonds in proteins and peptides. *Biochim. Biophys. Acta* **1973**, *303*, 14.

(35) Blumenstein, M.; Layne, P. P.; Najjar, V. A. NMR studies on the structure of the tetrapeptide Tuftsin, Thr-Lys-Pro-Arg and its pentapeptide analogue Thr-Lys-Pro-Pro-Arg. *Biochemistry* **1979**, *18*, 5247–5253.

(36) Konopinska, D.; Nawrocka, E.; Siemion, I. Z.; Szymaniec, S.; Slopek, S. In *Peptides*; Loffet, A.; Ed.; Editions de l'Universitē de Bruxelle: Belgique, 1976; pp 535–539.

(37) Chipens, G.; Nikiforovich, G.; Mutulis, F.; Veretennikova, N.; Vosekalna, L.; Sosnov, S.; Polevayz, L.; Ancans, J.; Mishlakova, N.; Liepinsh, E.; Sekacis, I.; Breslav, M. *Peptides: Structure and Biological Function*; Proceedings of the 6th American Peptide Symposium; Gross, E., Meienhofer, Y.; Eds.; Pierce Chemical Company 1979; pp 567–570.

(38) Pettitt, B. M.; Karplus, M.; Rossky, P. J. An Integral Equation Model for Aqueous Solvation of Polyatomic Solutes. *J. Phys. Chem.* **1986**, *90*, 6335–6345.

(39) Mezei, M.; Mehrotra, P. K.; Beveridge, D. L. Monte-Carlo Determination of the free energy and internal energy of hydration for the Ala dipeptide at 25 C. *J. Am. Chem. Soc.* **1985**, *107*, 2239–2245.

(40) Stabinsky, Y.; Gottlieb, P.; Fridkin, M. The phagocytosis stimulating peptide Tuftsin: a further look into structure–function relationships. *Mol. Cell. Biochem.* **1980**, *30*, 165–170.

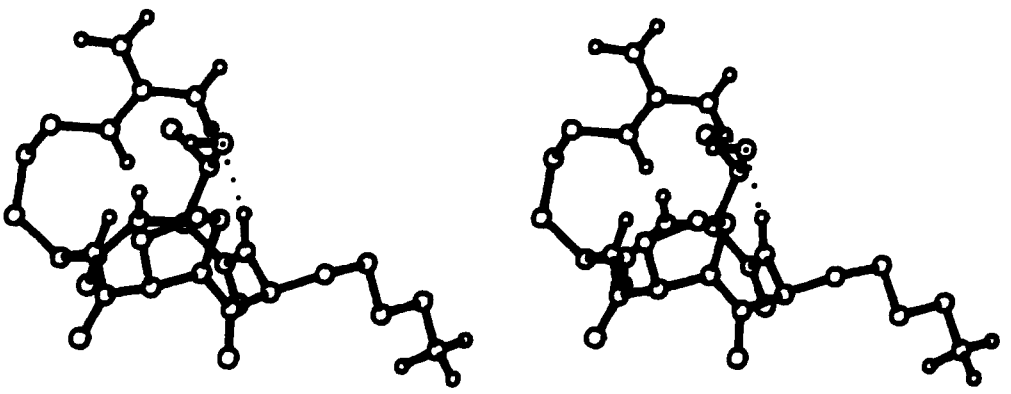

Figure 9. Stereo plot of a representative structure for $ctuf_1$ in water generated by quenched molecular dynamics.

residue ($ctuf_3$) increases the net charge on the peptide to +3, whereas the addition of an Asp residue ($ctuf_4$) reduces the net charge to +1. Both of these additions represented conservative substitutions in the Fc portion of leukokinin.

Each of the four analogues was studied using QMD. The low-energy families obtained were then compared to the linear tuftsin families to see if they possessed the same conformational characteristics. As for linear tuftsin, certain analogues were studied in both DMSO and aqueous solvents.

(1) **$Ctuf_1$ (Cyclo[Thr-Lys-Pro-Arg]).** Upon analysis of the 150 resulting structures obtained for $ctuf_1$ in DMSO, 22 structures were found within 3.5 kcal/mol of the lowest energy conformer and were considered for further analysis. Examination of the populated ϕ,ψ and χ^1,χ^2 conformers from each of the 22 selected structures indicated a rigid, strained cyclic framework. Grouping the 22 structures into families, based on the rms differences between the C^α–C segments of the various conformers, gave just one major family (Table IV). The overall backbone conformation was a type III β-turn (see Figure 8), with the only differences between members of the same family appearing in the orientation of their side chains. The presence of a hydrogen bond between Thr-1 OH and Lys-2 NH was also observed in these structures and can be related to the rigidity of the small lactam ring. The backbone conformation restricted the side chains of Thr-1 and Pro-3 to the same conformation in all the structures. The rigidity of the templet backbone also restricted the flexible side chains of Lys-2 and Arg-4 to the g^- and t conformations (Table IV).

The simulation of $ctuf_1$ in a continuum aqueous solvent produced 25 selected structures within 3.5 kcal/mol of the energy minimum. Classification of these structures according to the rms differences between their C^α–C segments again produced only one major family (Table IV). The type III β-turn backbone conformation adopted by $ctuf_1$ in water was identical to that of $ctuf_1$ in DMSO. Some minor differences were found in the side-chain orientations of Lys-2 and Arg-4 (Table IV, Figures 8 and 9). Within the same family, all the structures displayed similar backbone conformations, with the only significant differences lying in the orientation of the side chains. Upon graphical examination of a few selected cyclic tuftsin conformers it appeared that there was a larger degree of side-chain motion in the aqueous environment compared to that in DMSO. This behavior is supported by NMR studies of linear tuftsin in DMSO.[35] There were no major backbone conformational changes in the cyclic tuftsin structure when simulated in either DMSO or aqueous solvent environments.

Table IV. Representative Dihedral Angles of $ctuf_{1-3}$ from Quenched Molecular Dynamics

residue	dihedral	$ctuf_1$ (DMSO) F1	$ctuf_1$ (water) F1	$ctuf_2$ F1	$ctuf_3$ F1
Thr-1	ϕ	-82	-85	-90	-83
	ψ	-63	-61	-57	-73
	χ^1	53	54	-59	52
	χ^2	-59	-57	60	179
Lys-2	ϕ	-97	-103	-156	-119
	ψ	-43	-43	123	-45
	χ^1	-62	-62	52	-65
	χ^2	177	-64	-176	180
Pro-3	ϕ	-82	-77	-86	-73
	ψ	-56	-58	-15	-47
	χ^1	-23	-28	37	-25
Arg-4	ϕ	-98	-105	-94	-139
	ψ	-49	-39	-59	-29
	χ^1	-58	68	-62	32
	χ^2	-63	-73	-66	61
Gly-5 or Lys-5	ϕ			-81	-128
	ψ			-78	-54
	χ^1				-174
	χ^2				-175
no. in family		22	25	22	26
energy (kcal/mol)		7.48	6.33	-5.20	-9.56

A comparison of the conformational properties of $ctuf_1$ with those of linear tuftsin suggested major differences between both their backbone and side-chain conformations. Thus, if one of the predicted conformational families of linear tuftsin represents the bioactive conformation, synthesis and bioassay of $ctuf_1$ should result in reduced activity compared with the parent compound. An experimental study of $ctuf_1$ could confirm or refute the validity of the predicted conformations of both linear and cyclic tuftsin.

(2) **$Ctuf_2$ (Cyclo[Thr-Lys-Pro-Arg-Gly]).** Examination of the ϕ,ψ and χ^1,χ^2 dihedral angle maps for all the energy-selected structures of $ctuf_2$ (not shown) displayed a somewhat broader distribution than for $ctuf_1$. These structures were all very similar and produced only one rms family (Table IV and Figure 10). A type IV β-turn at the Lys-Pro position was observed in all of the structures while they displayed slight differences in conformation between the ϕ angle of Arg-4 and the ψ angle of Gly-5. Eight of the structures exhibited a type III β-turn at Arg-Gly, while 14 displayed a type II β-turn at the Arg-Gly segment. The existence of multiple conformations for the Arg-Gly turn

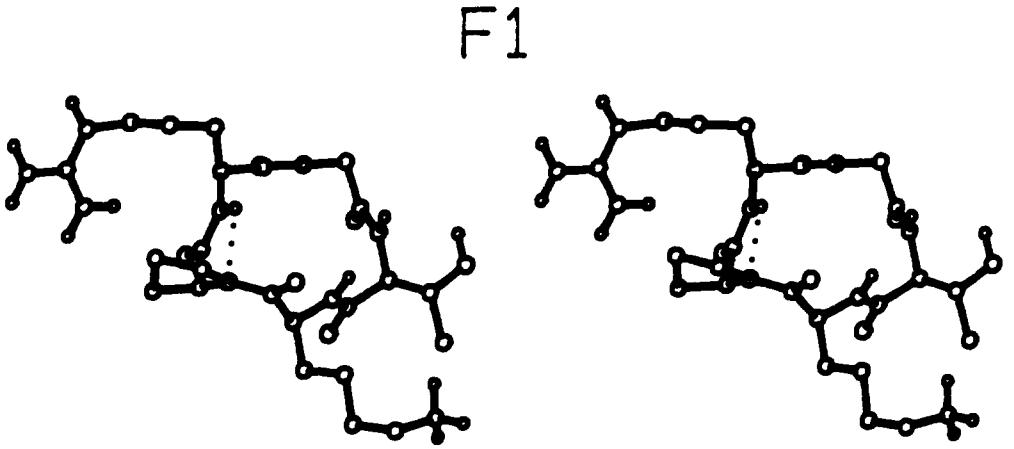

Figure 10. Stereo plot of a representative structure for $ctuf_2$ in DMSO generated by quenched molecular dynamics.

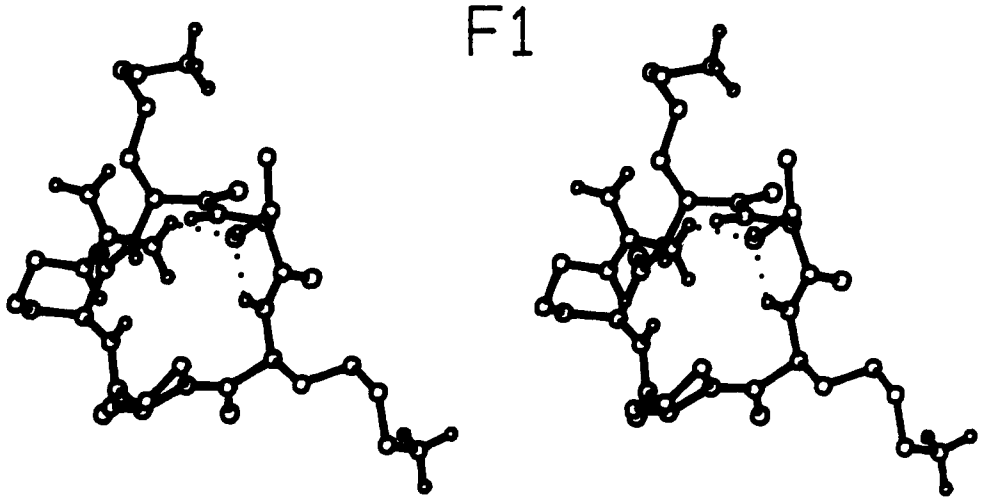

Figure 11. Stereo plot of a representative structure for $ctuf_3$ in DMSO generated by quenched molecular dynamics.

was probably related to the flexibility of glycine, which can span the broadest range of conformational space.[34] In order to determine the importance of the Arg-Gly turn for biological activity a D amino acid could be substituted for Gly, thereby enhancing the existence of type II β-turns.[41] The synthesis and biological testing of both cyclo[Thr-Lys-Pro-Arg-Gly] and cyclo[Thr-Lys-Pro-Arg-(D)Xxx] would aid in determining the most probable bioactive conformation and the associated topography.

Further examination revealed that the only differences between most of the structures appeared in the conformations of their amino acid side chains and mainly at the Lys-2 and Arg-4 positions (Figure 10). In addition, the existence of a type IV β-turn at the Lys-Pro position was correlated to the linear tuftsin conformation, as reported earlier. Thus, $ctuf_2$ appears to be a good candidate to synthesize and test for phagocytosis activity.

(3) $Ctuf_3$ (Cyclo[Thr-Lys-Pro-Arg-Lys]). $Ctuf_3$ was studied in order to understand the conformational effects of replacing Gly-5 of $ctuf_2$ with other charged amino acids. The substitution of Lys for Gly modified the total charge on the peptide from +2 to +3, and allowed us to investigate the effects that an additional positive charge had on the conformations available to the peptide in solution. The results are presented in Table IV and Figure 11. Examination of the various structures revealed that the presence of Lys-5 in the macrocycle favored a type III β-turn conformation at the Lys-Pro position and a type I β-turn at either the Arg-Lys or Lys-Thr positions. This change in conformation, relative to native tuftsin and $ctuf_2$ (type IV β-turn), may be related to the presence of either lysine, which prefers to exist in a β-turn conformation,[42] or the extra positive charge present in $ctuf_3$. All of the structures displayed similar backbone conformations with the major variations occurring in the side-chain orientations and, to a lesser extent, the hydrogen-bonding patterns. It has been reported that addition of Lys (e.g., Lys-Thr-Lys-Pro-Arg)[43] to the straight-chain peptide results in a large loss in biological activity. This finding is consistent with the conformational hypothesis suggested by our work on linear tuftsin. Therefore, based on this study, this method predicts that the cyclic analogue $ctuf_3$ will also exhibit little or no biological activity.

(4) $Ctuf_4$ (Cyclo[Thr-Lys-Pro-Arg-Asp]). To further investigate the effect of replacing the Gly of $ctuf_2$ with other amino acids, $ctuf_4$ was designed and its conformational properties were investigated. The addition of Asp-5 reduced the net charge on $ctuf_4$ to +1. This allowed us to consider the effects that reducing the total positive charge had on the conformation of tuftsin, just as $ctuf_3$ reflected any effects due to an increased positive charge. The results are presented in Table V and Figure 12. Classification of the 22 resulting conformers of $ctuf_4$ was completed as before and produced two families of conformers (Table V).

(41) Rose, G. D.; Gierasch, L. M.; Smith, J. A. Turns in peptides and proteins. *Adv. Protein Chem.* **1985**, *37*, 1-109.

(42) Chou, P. Y.; Fasman, G. D. Empirical predictions of protein conformation. *Annu. Rev. Biochem.* **1978**, *47*, 251-276.

(43) Sucharda-Sobczyk, A.; Siemion, I. Z.; Konopinska, D. Infrared Spectroscopic Investigation of Tuftsin and its analogs. *Eur. J. Biochem.* **1979**, *96*, 131-139.

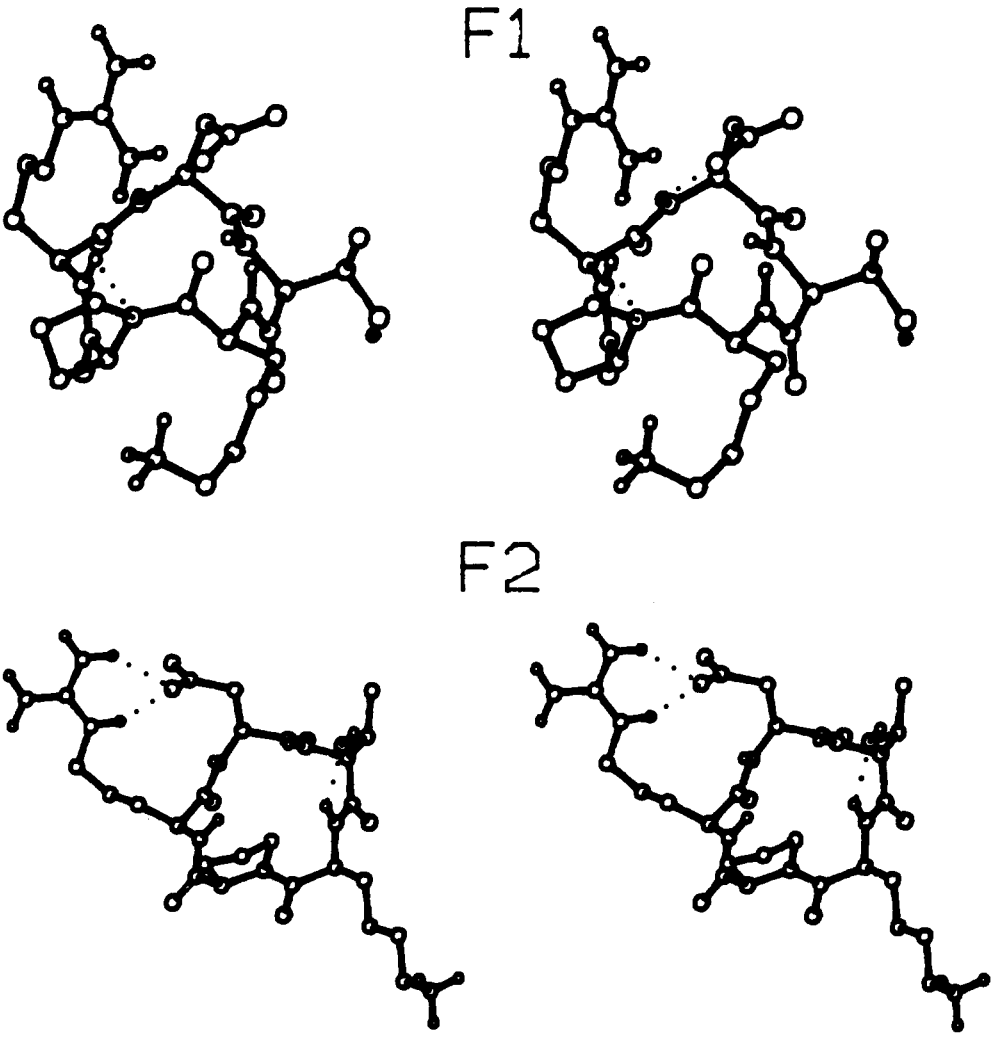

Figure 12. Stereo plots of representative structures from families 1 and 2 $ctuf_4$ in DMSO generated by quenched molecular dynamics.

Examination of the conformations from the selected families revealed that family 1 displayed a type IV β-turn at the Lys-Pro position and a type III β-turn at the Arg-Asp position. Family 2 had a similar conformation at the Arg–Asp position; however, these conformers also possessed a type III β-turn at Lys-Pro. Hence, all of the structures displayed similar conformations for the lactam ring but differed in the Lys-Pro region. Furthermore, the structures within the families differed only in their side-chain conformations and the number of intramolecular hydrogen bonds present (Table V and Figure 12). Thus, $ctuf_4$ displayed many conformational features which were similar to linear tuftsin. Synthesis and biological studies, as well as further conformational studies, will provide some insight as to the validity of the method for predicting possible conformation(s) in solution.

Conclusions

We have devised and tested a particular form of high-temperature quenched molecular dynamics designed to expore the width of the thermally accessible conformational space rather than to locate a single low-energy structure. Due to the availability of experimental data, and the existence of superpotent cyclic analogues, our major control study centered on well-studied peptides with opiate activity. Using QMD, and starting with an extended conformation of Met-enkaphalin, we were able to locate families of structures which are probably representative of the conformations of Met-enkephalin in solution. Two of these families had comparable structures (rms $\approx$ 1.5 Å) to the known structure of a potent cyclic analogue of Met-enkephalin. Appropriate derivatization and cyclization of these structures would produce comparable structures to the analogue. These observations indicate that this method should have a large range of validity and suggest that, under favorable conditions, the results from quenched dynamics simulations may be used with confi-

Table V. Representative Dihedral Angles of $ctuf_4$ from Quenched Molecular Dynamics in DMSO

residue	dihedral	F1	F2
Thr-1	ϕ	-154	-94
	ψ	-36	-65
	χ^1	-178	53
	χ^2	61	180
Lys-2	ϕ	-153	-122
	ψ	111	-46
	χ^1	-174	-173
	χ^2	65	-179
Pro-3	ϕ	-88	-69
	ψ	-19	-42
	χ^1	36	-27
Arg-4	ϕ	-103	-146
	ψ	-44	-55
	χ^1	68	-173
	χ^2	-71	-170
Asp-5	ϕ	-80	-88
	ψ	-44	-57
	χ^1	60	-53
	χ^2	-52	96
no. in family		14	8
energy (kcal/mol)		-8.31	-6.83

dence to predict good cyclic analogues of linear peptides.

The conformational study of linear tuftsin suggested the presence of a type IV β-turn at the Lys-Pro position. This information combined with previous experimental/synthetic studies led us to propose four cyclic analogues of tuftsin. Quenched dynamical searches of the conformational space of the four proposed cyclic tuftsin analogues revealed the following: direct cyclization of tuftsin through the N and C termini, as in $ctuf_1$, resulted in a complete loss of the conformational characteristics (type IV β-turn) of the linear tuftsin. Also, addition of Lys at position 5 prior to cyclization, as in $ctuf_3$, resulted in a different conformation relative to the linear tuftsin. However, addition of either Gly or Asp at position 5 ($ctuf_2$ and $ctuf_4$, respectively) resulted in a similar backbone conformation (type IV β-turn) at Lys-Pro. Also, side-chain conformations of $ctuf_2$ and $ctuf_4$ displayed most of the characteristics of the linear analogue. Thus, using the strategy outlined here, we conclude that $ctuf_2$ and $ctuf_4$ are the most reasonable candidates for synthesis and biological testing (K. Nishioka, work in progress). These studies will provide some further insight on the validity of these particular theoretical methods.

Acknowledgment. We would like to thank Prof. V. J. Hruby and Prof. K. Nishioka for numerous interesting discussions and the Robert A. Welch Foundation and the National Institutes of Health for partial support.

Note Added in Proof: K. Nishioka has performed experiments which indicate that $ctuf_2$ is 50 times more potent than tuftsin in a phagocytosis assay.

Registry No. Tyr-Gly-Gly-Phe-Met, 58569-55-4; Thr-Lys-Pro-Arg, 9063-57-4; cyclo(Thr-Lys-Pro-Arg), 83797-39-1; cyclo(Thr-Lys-Pro-Arg-Gly), 140175-51-5; cyclo(Thr-Lys-Pro-Arg-Lys), 140175-52-6; cyclo(Thr-Lys-Pro-Arg-Asp), 140175-53-7; (*S*)-$C_3H_3CHBrCH_2CH_3$, 5787-32-6.

Nucleosides and Nucleotides. 112. 2-(1-Hexyn-1-yl)adenosine-5′-uronamides: A New Entry of Selective A_2 Adenosine Receptor Agonists with Potent Antihypertensive Activity[1]

Hiroshi Homma,[†] Yohko Watanabe,[‡] Toichi Abiru,[‡] Toshihiko Murayama,[†] Yasuharu Nomura,[†] and Akira Matsuda*,[†]

Faculty of Pharmaceutical Sciences, Hokkaido University, Kita-12, Nishi-6, Kita-ku, Sapporo 060, Japan, and Research Laboratories, Yamasa Shoyu Company, Ltd., Araoicho 2-10-1, Choshi-shi, Chiba 288, Japan. *Received February 24, 1992*

Chemical modifications of the potent A_2 adenosine receptor agonist 2-(1-hexyn-1-yl)adenosine (**7**, 2-HA) at the 5′-position have been carried out to find more potent and selective A_2 agonists. These analogues were evaluated for adenosine A_1 and A_2 receptor binding affinity in rat brain tissues and antihypertensive effects in spontaneously hypertensive rats (SHR). Among the series of compounds, 2-(1-hexyn-1-yl)adenosine-5′-*N*-cyclopropyluronamide (**16d**) had the most potent affinity to the A_2 receptor with a K_i of 2.6 nM, which is essentially the same as that of the parent agonist, 2-HA. However, the most selective agonist for the A_2 receptor was 2-(1-hexyn-1-yl)-adenosine-5′-*N*-methyluronamide (**16b**) with a K_i of 11 nM and a 162-fold selectivity. The *N*-alkyl substituents of 5′-uronamide derivatives did not seem to potentiate the A_2 binding affinity but drastically reduced the A_1 affinity compared with the parent 2-HA. Therefore, the A_1/A_2 selectivity was consequently increased. Other 5′-deoxy-5′-substituted derivatives of 2-HA such as the chloro (**20**), carboxamide (**27**, **28**), sulfonamide (**29**), urea (**30**), and thiourea (**22**) analogues were also prepared. Among these nucleosides, no active compounds with potent or selective affinities to both receptors were found except **20**. Although glycosyl conformations and sugar-puckering of these nucleosides were studied by ^1H NMR spectroscopy, there were no positive correlations between active and inactive agonists. 2-(1-Hexyn-1-yl)adenosine-5′-uronamide (**16a**) and **16d** had a potent hypotensive effect at ED_{30} values of 0.18 and 0.17 μg/kg, respectively, upon iv administration to anesthetized SHR.

There is considerable evidence to indicate that adenosine derivatives specifically modulate coronary vasodilation via one of the cell surface adenosine receptors, termed A_2, which mediates stimulation of intracellular cAMP accumulation.[2] Selective A_2 adenosine receptor agonists elicit antihypertensive activity in rats while analogues having preferential binding affinity for the A_1 receptor produce depression in heart rate and cardiac contractility, which is considered to be a side effect for antihypertensive agents.[3] Therefore, selective A_2 receptor agonists have a potential for the treatment of cardiovascular diseases with minimized toxic effects.

Recently, several A_2 selective agonists, such as N^6-[2-(3,5-dimethoxyphenyl)-2-(2-methylphenyl)ethyl]adenosine (**3**, DPMA),[4] 2-[[4-(2-carboxyethyl)phenethyl]amino]-adenosine-5′-*N*-ethyluronamide (**4**, CGS 21680),[5] 2-[2-(4-methylphenyl)ethoxy]adenosine (**5**, MPEA),[6] and 2-[(2-cyclohexylethyl)amino]adenosine (**6**, CGS 22492),[7] which are shown in Chart I along with classical standards, have been reported. We have also reported that 2-alkynyl-

* Author to whom correspondence should be addressed.
† Hokkaido University.
‡ Yamasa Shoyu Co., Ltd.

(1) Part 111: Nishio, H.; Ono, A.; Matsuda, A.; Ueda, T. Thermal stability of oligodeoxyribonucleotide duplexes containing N^6-hydroxyladenine in substitution for adenine. *Chem. Pharm. Bull.* **1992**, *40*, 1355-1357.
(2) Haleen, S. J.; Evans, D. B. Selective effects of adenosine receptor agonists upon coronary resistance and heart rate in isolated working rabbit hearts. *Life Sci.* **1985**, *36*, 127-137.
(3) Hutchison, A. J.; Webb, R. L.; Oei, H. H.; Ghai, G. R.; Zimmerman, M. B.; Williams, M. CGS 21680C, an A_2 selective adenosine receptor agonists with preferential hypotensive activity. *J. Pharmacol. Exp. Ther.* **1989**, *251*, 47-55.
(4) Bridges, A. J.; Bruns, R. F.; Ortwine, D. F.; Priebe, S. R.; Szotek, D. L.; Trivedi, B. K. N^6-[2-(3,5-Dimethoxyphenyl)-2-(2-methylphenyl)ethyl]adenosine and its uronamide derivatives. Novel adenosine agonists with both high affinity and high selectivity for the adenosine A_2 receptor. *J. Med. Chem.* **1988**, *31*, 1282-1285.
(5) Hutchison, A. J.; Williams, M.; de Jesus, R.; Yokoyama, R.; Oei, H. H.; Ghai, G. R.; Webb, R. L.; Zoganas, H. C.; Stone, G. A.; Jarvis, M. F. 2-(Arylalkylamino)adenosine-5′-uronamides: A new class of highly selective adenosine A_2 receptor ligands. *J. Med. Chem.* **1990**, *33*, 1919-1924.

0022-2623/92/1835-2881$03.00/0